Proceedings of the INMM & ESARDA Joint Virtual Annual Meeting
August 23–26 & August 30–September 1, 2021

HYBRID K-EDGE ANALYSIS: MULTI-ELEMENTAL KED AND XRF ANALYSIS CHALLENGES

Robert D. McElroy Jr.
Oak Ridge National Laboratory

Susan Smith
Oak Ridge National Laboratory

ABSTRACT

Hybrid x-ray fluorescence and K-edge densitometry (KED) is used at nuclear fuel reprocessing facilities to determine the concentrations of uranium and plutonium in the input accountability vessel. The uranium concentration is determined by KED, that is, from the step-difference in transmission on either side of the K-absorption edge measured using a continuous x-ray spectrum on a vial of the solution defining a well-known geometry. In parallel with the transmission measurement, the relative plutonium-to-uranium concentration is obtained from the relative strength of the x-ray–induced K-shell x-ray fluorescence production measured at a backward angle in energy-dispersive mode. The HKED analysis method has recently been extended to accommodate more complex solutions providing concentration values for an arbitrary mixture of actinides representative of the evolving nuclear fuel cycle. The extension to these solutions and the correspondingly complex spectra has been hampered by challenges in accurately representing the backscatter Bremsstrahlung spectrum, correcting for self-irradiation effects from high fission product loadings, predicting the relative fluorescence yields and limitations in the available atomic data (e.g., mass attenuation coefficients). This work discusses the impact of these challenges on the HKED measurement and Oak Ridge National Laboratory's efforts to address them.

INTRODUCTION

The Hybrid K-edge Densitometer (HKED) developed by Ottmar and Eberle [1] has long been a key element of international safeguards for accountancy of uranium and plutonium in dissolver and product solutions associated with the reprocessing of spent nuclear fuel. The HKED provides simultaneous K-edge densitometry (KED) and x-ray fluorescence (XRF) spectroscopy of small volume samples (<5 mL) of dissolver solutions from nuclear fuel reprocessing facilities. The uranium concentration determined by the KED measurement is highly accurate, providing measurement precision and bias of 0.1–0.3% for concentrations between 100 and 400 g U/L. The XRF measurement provides the concentrations of minor actinide constituents of the sample relative to the uranium concentration. The performance of the XRF measurement for typical dissolver solutions with U:Pu concentration ratios of 100:1 is generally limited by its statistical precision to 0.5–0.7% for the Pu contents for a 1 hour measurement time.

The HKED system was introduced in the late 1980s; at that time the XRF component of the hybrid analyses was limited to quantification of uranium and plutonium for a narrow range of U:Pu concentration ratios in the vicinity of ≈100. The evolving nuclear fuel cycle created the need to assay more complex dissolver solutions in which uranium may no longer be the dominant actinide in the solution, and the concentrations of the minor actinides (e.g., Th, Np, Am, and Cm) are sufficiently high that they can no longer be treated as impurities or ignored. Oak Ridge National Laboratory (ORNL) developed a spectral fitting approach to the HKED XRF measurement with an enhanced algorithm set to accommodate these complex XRF spectra [2], [3], [4], [5]. Several challenges arose during this development activity and still persist. These are the

quality of the mass attenuation coefficients available for the actinides, the complexity of the backscattered Bremsstrahlung spectrum, and development of a more convenient correction for self-irradiation. The impact of each of these challenges on the performance of the HKED analysis are discussed below.

MASS ATTENUATION COEFFICIENTS

A primary objective for the multi-elemental K-edge transmission measurement is to eliminate the need for calibration standards by creating a first principles analysis methodology. This was achieved by identifying all source terms contributing to the measured spectrum, and correcting for attenuation and detector specific response functions. Unlike the historical KED analysis [1], the multi-elemental K-edge analysis does not rely on a reference blank. The multi-elemental analysis is based on an analytical model of the transmission spectrum. The shape and intensity of the x-ray distribution emitted from the generator are determined from the observed transmission spectrum. The accuracy of the Multi-Elemental K-edge densitometer (MEKED) measurement is presently limited by the uncertainties in the mass attenuation coefficients available for the actinides. The MEKED analysis makes use of the values from the XCOM database [6]. The stated uncertainties of the attenuation data available from the database for the actinides is 1–2% [7] over the range of energies (60–160 keV) used in the MEKED analysis. The MEKED measurement provides measurement precision of <0.2% within the typical 1-hour measurement time; however, accuracy is limited by the XCOM data. Although intended as a purely physics-based analysis, without improved attenuation there will continue to be a need to calibrate the MEKED measurement using certified reference materials.

We have analyzed the KED spectra obtained from several HKED systems located at different laboratories using the MEKED method to evaluate the available mass attenuation coefficients for uranium and plutonium. Because the concentrations of the solutions were declared, with each facility using destructive analyses for their own materials, the results from each facility are considered independent. Comparison of the average MEKED analysis results for each facility allows us to estimate the average bias in the attenuation coefficients. The average biases for the uranium concentrations are presented in Table 1. The errors in the table assume a systematic uncertainty in the declared values for each facility. A similar bias has been observed for the plutonium concentration measurements.

Table 1. MEKED measurement bias using the XCOM mass attenuation coefficients for U.

	Average Bias in [U]
HKED System 1	1.0095 ± 0.0032
HKED System 2	1.0079 ± 0.0033
HKED System 3	1.0096 ± 0.0033
HKED System 4	1.0117 ± 0.0051
Weighted Average	1.0100 ± 0.0018

The observed 1% bias is consistent with the stated uncertainty for the XCOM data. However, this bias can be corrected in several ways. The mass attenuation coefficients from the XCOM database for the principal materials located between the x-ray generator and detector are shown in Figure 1. Over the relevant energy range, the actinide attenuation coefficients display the prominent jump at the K-edge transition while the attenuation coefficient curves for each element show a unique energy dependence. The observed bias can be corrected simply by multiplying the attenuation values by a constant factor, or by applying a scaling factor to the attenuation values for energies greater than the K-edge (i.e., increasing the height of the step). Alternatively, it is possible that the bias is related to the general shape of the attenuation coefficient curve.

We have attempted to develop attenuation coefficients from the HKED data [3]. To minimize the impact of the attenuation introduced by the HKED system (e.g., beam filters, detector endcap), the background-corrected KED transmission spectra from two solutions of differing uranium or plutonium concentrations

were ratioed. Figure 2 provides a comparison of the measured attenuation coefficients for plutonium with the XCOM cross section data scaled by a factor of 1.01194. A gaussian smoothing function has also been applied to the XCOM data to simulate the effect of the HPGe detector. The scaled XCOM data and the measured Pu attenuation coefficients agree very well for energies greater than 110 keV, but at lower energies the precision of the KED spectra degrades so it is not possible to determine definitively if the calculated XCOM energy dependence represents the actual coefficients over the entire energy range of interest.

We have noted a bias between mixed oxide and pure plutonium solutions after applying the correction to the attenuation coefficients. This residual bias suggests there is an energy-dependent component that is not accommodated by the simple scaling factors. However, until improved attenuation coefficient data are available for uranium and plutonium, we have opted to apply the bias corrections as simple multipliers across the entire energy range.

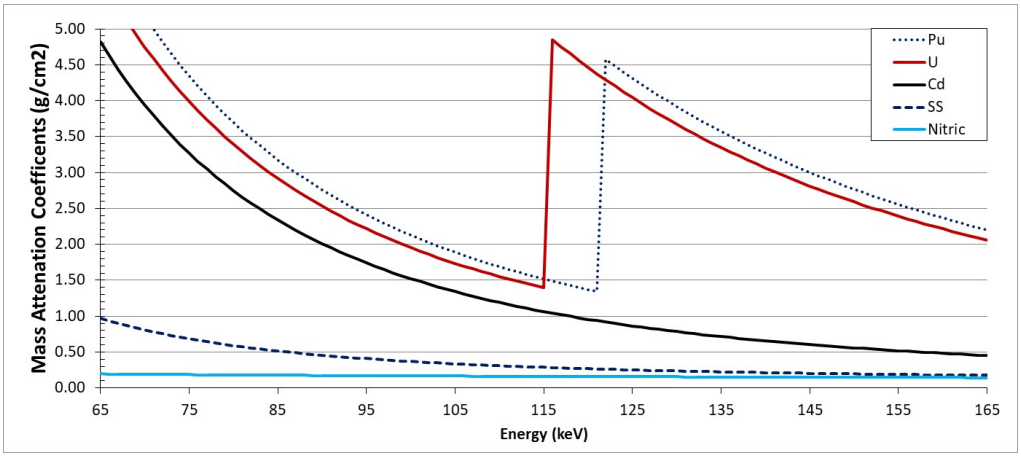

Figure 1. Plot of the total mass attenuation coefficients, obtained from the XCOM database [6], for several materials present in the HKED system over the energy range of interest to the MEKED analysis.

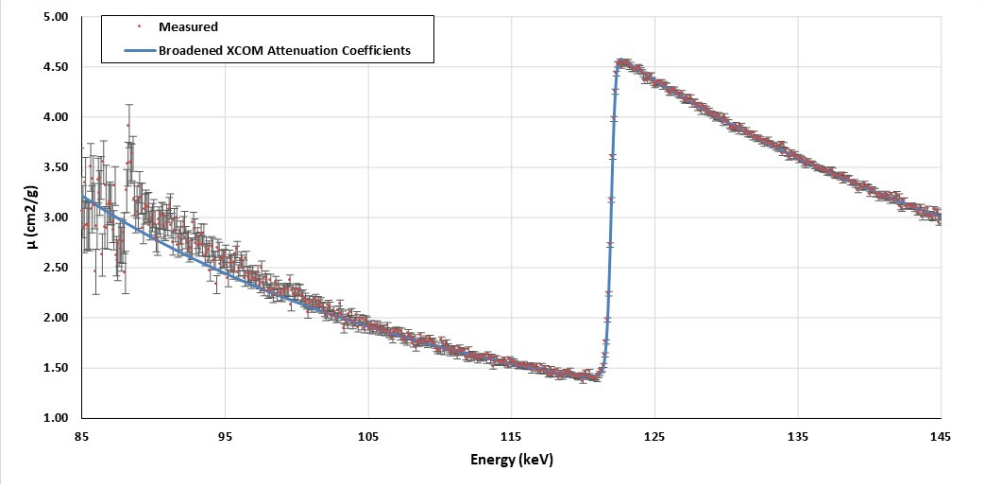

Figure 2. Plot of the measured plutonium mass attenuation coefficient as a function of energy, determined by ratio of the net response from two plutonium nitrate solutions. Scattering events within the system and the high-purity germanium detector as well as the presence of the ^{109}Cd reference peak introduce an interference with the measurement below 105 keV.

REPRESENTATION OF THE BACKSCATTERED BREMSSTRAHLUNG FOR THE XRF ANALYSIS

Representation of the transmitted x-ray spectrum as a function of energy through the sample vial for the MEKED analysis is relatively straightforward. Although there are many constants and free variables impacting the spectrum, each component is readily identifiable and well described. The backscatter spectrum of the XRF measurement is more complex and is more highly dependent on the mechanical design of the HKED system, and in addition the random coincidence contribution has greater impact on the analysis. The primary components of the backscatter spectrum are the elastically scattered, inelastically scattered, and multiply scattered x-rays from the generator. While the elastically and inelastically scattered distributions, as well as the random coincidence contribution are well described analytically, the multiply scattered component is not. The challenge in representing the contribution from multiple scattering events arises from the distributed nature of the spatial origin of the x-rays. The various contributions are shown in Figure 3 for a low concentration (< 5 g/L) U–Pu solution. To provide an accurate analysis of the characteristic x-ray distribution, it is necessary to accurately describe the continuum beneath the peaks.

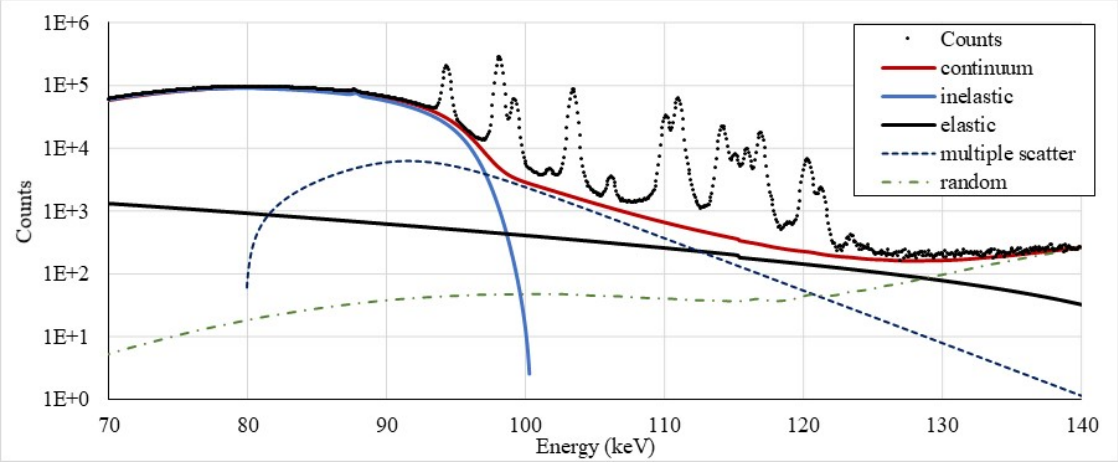

Figure 3. Plot illustrating the contributions to the MEXRF backscatter continuum.

To illustrate the complexity of the multiply scattered x-ray contribution to the continuum, we consider the simplest case where the x-ray scatters only twice. At each scattering event, the photon may scatter elastically or inelastically, and with each inelastic scattering event the energy of the x-ray is reduced. The resulting x-ray energy is dependent on the initial energy and the angle of scatter relative to its initial direction. As illustrated in Figure 4, the potential paths of the scattered x-ray must eventually take it through the XRF detector's collimator, but the overall distance traveled though the sample vial changes with the scattering angle, as do the mass attenuation coefficients for the scattered photon as its energy has changed. It is possible to calculate the resulting probability distribution as a function of energy for x-rays reaching the detector; however, the process is computationally intensive and would result in impractically long analysis times for the XRF analysis.

Although an overriding tenet for the MEKED analysis was to provide a first principles approach eliminating the need for calibration, the challenge of calculating the multiple scattering contribution to the continuum forced adoption of an empirical representation for these photons in the MEXRF analysis. The functional form selected is justified only in that it provides a reasonable representation of the necessary response function (i.e., because it works). The functional form for the multiple scatter contribution, I_{MS} is given by

$$I_{MS} = \frac{a_1}{\cosh\left((E-E_1)/\tau\right)} + \frac{a_2}{\cosh\left((E-E_2)/\tau\right)},$$

where E is the energy of the detected photon and the parameters, a_1, a_2, E_1, E_2, and τ are determined during the fitting process. The functional form is illustrated in Figure 3. However, because this is a purely empirical

representation, as the measurement precision improves (e.g., for long measurement times) systematic deviations between the measured spectra and the calculated response function become apparent. Although this deviation does not adversely impact the measurement performance for routine assay times (1,000–3,000 seconds), it may be a limiting factor in measurement precision.

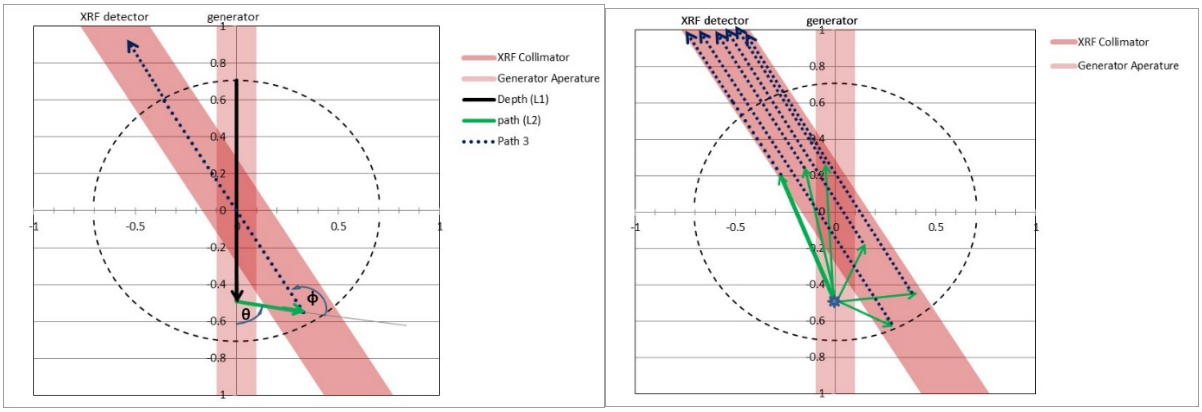

Figure 4. Illustration of the various paths to the XRF detector for x-rays undergoing multiple scattering with the sample vial. (A single path is shown on the left, while the plot on the right illustrates multiple potential scatter paths from a single interaction point.)

XRF SELF-IRRADIATION CORRECTIONS

Dissolver solutions contain fission product loadings on the order of 3×10^{12} Bq/L (100 Ci/L). The decay of these fission products will produce K-shell vacancies in the actinides causing a passive XRF signal from the sample (Figure 5). This self-irradiation effect results in a typical bias in U:Pu ratio on the order of 0.3% if no correction is performed. The self-interrogation effect has historically been corrected by means of a passive background subtraction. The correction, although accurate, is time-consuming and typically several hours in duration adversely impacting the throughput of the HKED system. We have attempted to extend the multi-elemental XRF algorithm set to provide a correction for self-irradiation effects without the need for a time-consuming passive measurement [8].

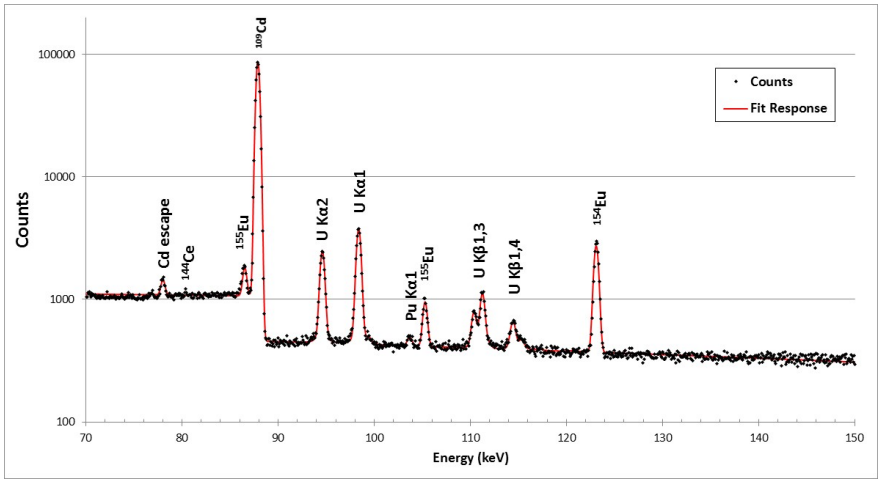

Figure 5. Passive XRF spectrum from an HKED dissolver solution measurement [8].

The hybrid KED/XRF measurement determines the plutonium concentration relative to the uranium concentration determined using the KED transmission analysis. Reference [1] provides an expression for the U:Pu concentration ratio, which we have expanded to account for the various dependences of the U:Pu measurement [4] as

$$\frac{[U]}{[Pu]} = \frac{A_U}{A_{Pu}} \cdot \frac{I_{UK\alpha 1}}{I_{PuK\alpha 1}} \cdot \frac{\sum_i f_{PuKi} \cdot \varepsilon(E_{PuKi})}{\sum_i f_{UKi} \cdot \varepsilon(E_{UKi})} \cdot \frac{1}{R_{U/Pu}}, \tag{1}$$

where $I_{UK\alpha 1}$ is the count rate in the uranium $K_{\alpha 1}$ peak,
$I_{PuK\alpha 1}$ is the count rate in the plutonium $K_{\alpha 1}$ peak,
A_U and A_{Pu} are the atomic weights of uranium and plutonium, respectively,
$\varepsilon_{PuK\alpha 1}$ is the detection efficiency for the plutonium $K_{\alpha 1}$ x-ray,
$\varepsilon_{UK\alpha 1}$ is the detection efficiency for the uranium $K_{\alpha 1}$ x-ray,
$g(E)$ is the interrogating x-ray flux at the detectable interaction region of the sample vial,
f_{UK_i} is the relative yield for the i^{th} fluorescence x-ray (per K-shell vacancy) in uranium,
f_{PuK_i} is the relative yield for the i^{th} fluorescence x-ray (per K-shell vacancy) in plutonium,
$\varepsilon(E_{UKi})$ is the detection efficiency of the i^{th} fluorescence x-ray in uranium,
$\varepsilon(E_{PuKi})$ is the detection efficiency of the i^{th} fluorescence x-ray in plutonium,
$[U]$ is equal to the uranium concentration within the sample in grams per cubic centimeter, and
$[Pu]$ is equal to the plutonium concentration within the sample in grams per cubic centimeter.

The analysis of Reference [4] redefines the conversion factor, $R_{U/Pu}$, from Eq. 1 as

$$R_{U/Pu} = \iiint (1 + F_{U:Pu}) \cdot \frac{\int_0^{E_0} \cdot\, g(E) \cdot [U] \cdot \mu_{U,PE}(E) \cdot dE}{\int_0^{E_0} g(E) \cdot [Pu] \cdot \mu_{Pu,PE}(E) \cdot dE} dxdydz\,, \tag{2}$$

where $F_{U:Pu}$ is the relative uranium fluorescence rate due to the presence of higher Z actinides,
$g(E)$ is the interrogating x-ray flux at the detectable interaction region of the sample vial,
$\mu_{U,PE}$ is the K-shell photoelectric interaction coefficient for uranium, and
$\mu_{Pu,PE}$ is the K-shell photoelectric interaction coefficient for plutonium.

The function for the x-ray energy distribution, $g(E)$, incorporates the properties of the x-ray source and attenuation from all sources between the x-ray tube and the point where the K-shell vacancy is created.

In Reference [8], the decay of fission products within the dissolver solution introduces an additional source of production of actinide K-shell vacancies. In this case, the K-shell vacancies are produced uniformly throughout the sample, so the detectable region extends across the full diameter, *D*, of the vial. The conversion factor for the fission product created K-shell vacancy rates, $R_{\gamma,U/Pu}$, is determined by

$$R_{\gamma,U/Pu} = \int_0^D (1 + F_{U:Pu}) \cdot \frac{\int_0^{E_{max}} \cdot\, \gamma(E) \cdot [U] \cdot \mu_{U,PE}(E) \cdot dE}{\int_0^{E_{max}} \gamma(E) \cdot [Pu] \cdot \mu_{Pu,PE}(E) \cdot dE}\, dy, \tag{3}$$

where $\gamma(E)$ is the gamma-ray energy distribution within the sample and E_{max} is the highest gamma-ray energy of significance in the spectrum. The value of $R_{fp,U/Pu}$ required to calculate the relative concentration ratio [U]:[Pu] for the fission product loaded spectrum is then

$$R_{fp,U/Pu} = R_{U/Pu} + \frac{I_\gamma}{I_X} \cdot R_{\gamma,U/Pu}, \quad (4)$$

where I_γ and I_X are the relative intensities of the gamma-ray and x-ray fluences, respectively. A simulated photon energy distribution within the sample vial is provided in Figure 6. Note, although the typical fission product loading is on the order of 1E12 Bq/L, the gamma-ray fluence is small compared to that produced by the x-ray generator.

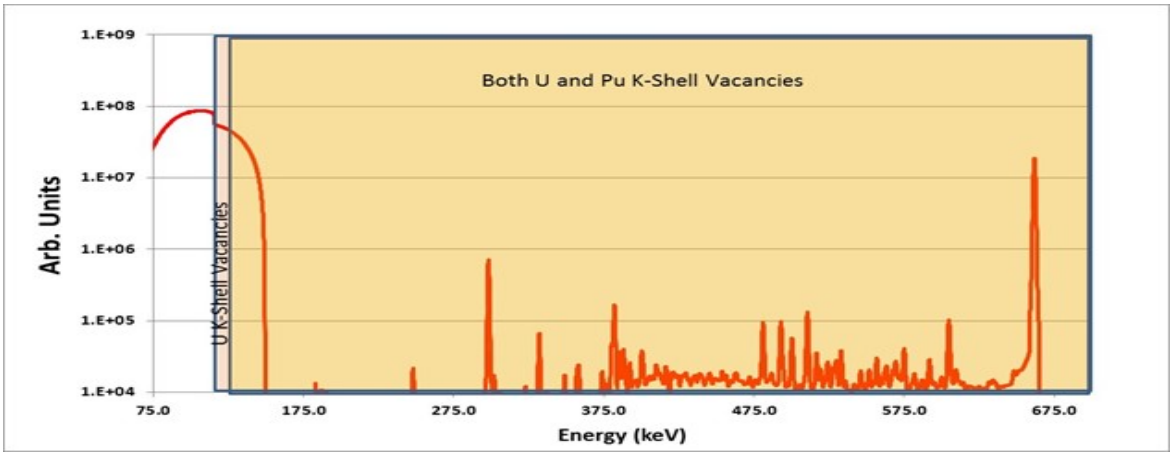

Figure 6. Illustration of the portions of the interrogating x-ray spectrum (simulated) that induce U and Pu K-shell vacancies. The notional spectrum is calculated for the interaction region at the center of the sample vial leading to detectable x-ray events for a solution containing 200 g U/L and 2 g Pu/L loaded with approximately 2E11 Bq/L fission products [8].

Determining the relative concentrations using the hybrid analysis requires an accurate determination of R_{UPu} (as well as for each of the other actinides; R_{UNp}, R_{UAm}, and R_{UCm}). To accomplish this, the fission product gamma-ray distribution must be determined relative to the interrogating x-ray distribution within the sensitive region of the sample vial. Unfortunately, the HKED systems in operation today are configured only to collect spectra up to ~180 keV, and the small planar detectors used for the HKED systems are not well suited for measurement of gamma rays in the 0.2–2 MeV energy range required for this analysis method.

CADMIUM-109 REFERENCE SOURCE

Both the KED and XRF detectors use a ^{109}Cd reference source for gain stabilization. The source is placed between the face of the detector cryostat and the tungsten shield. This presents multiple problems for the analyses. First, the peak shape and tailing properties of the ^{109}Cd characteristic 88 keV gamma-ray are not representative of the x-rays or gamma-rays emitted from within the sample vial. Second, random coincidences/pileup between the Kα x-rays from Ag and Cd with the 88 keV gamma-ray line create small peaks between 110 and 115 keV. If the ^{109}Cd source is strong enough, these peaks can interfere with both the XRF and KED measurements. The differing detector response for the reference gamma-ray peak and the x-ray distribution complicate removal of the pileup events. Finally, the intense peak tailing caused by the position of the ^{109}Cd source between the detector and the tungsten shield introduces a time-dependent behavior in the KED background correction. This occurs because the 88 keV peak tail extends through the background correction low energy region of interest [9].

Figure 7 shows a passive XRF spectrum acquired with the ORNL HKED system with no sample present. The ^{109}Cd source 88 keV peak rate was ~750 cps. Even with the digital signal processor's pileup reject active, ill-defined peaks are present at 100, 110, and 112.5 keV. These peaks act primarily as an interference for the XRF background determinations for both uranium and plutonium, as well as the americium peak

region of interest. For the ORNL system, these interferences were small, introducing a bias of ~25 mg/L. However, with different acquisition electronics and setup parameters, the peak locations may differ as much as 1 keV from the energies shown in the figure and may impact the peak area determinations differently. The pileup peaks in the 105–115 keV energy window fall within the low energy region of interest used for determination of the uranium concentration, resulting in an overestimation of the step change in the KED spectrum resulting in a slight positive bias that decreases with time.

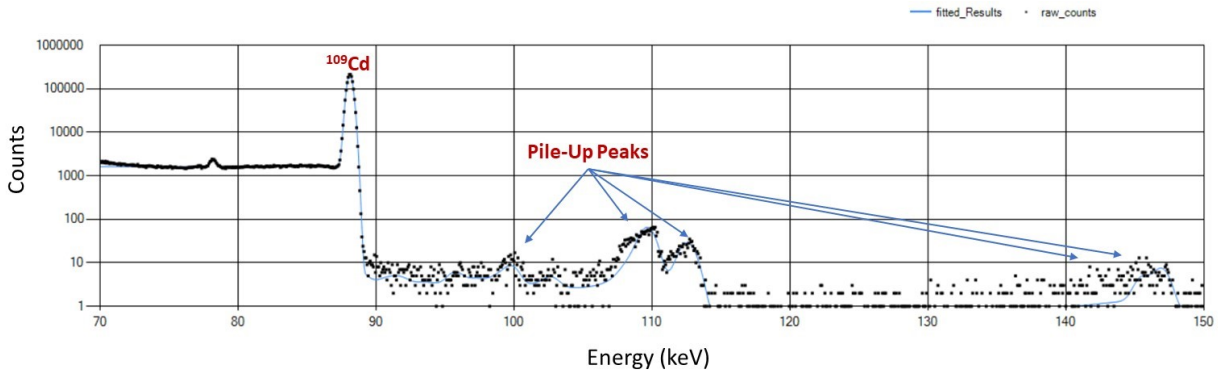

Figure 7. Spectrum from the ORNL XRF detector showing coincidence/pileup peaks due to the ^{109}Cd reference source. (Note, the pileup reject was active for this measurement.)

A more significant interference is the impact of the ^{109}Cd source on the background subtraction used for the KED transmission analysis. Figure 8 provides a comparison of the count rates in the energy region below the 88 keV line. The exponentially tailing step background from the reference source peak contributes to the count rate in the energy window used by the region of interest analysis method. As the reference source decays, the contribution to the background region of interest decreases, introducing a time-dependent bias into the KED transmission results. Estimates of the magnitude and time dependence of the bias are provided in Reference [9].

Lastly, the proximity of the 88 keV line to the Bi K-edge (90.53 keV) would prevent examination of the Bi content expected in certain reprocessing methods. Because of the number and complexity of the biases introduced by use of the ^{109}Cd reference source, an alternative stabilization source is recommended. A suitable replacement source would have a limited number of gamma-rays, each of which would have an energy exceeding 160 keV to preclude random coincidence summing, preferably with at least one gamma-ray between 160 and 200 keV. The source would preferably have a half-life greater than 1 year.

Elimination of the ^{109}Cd reference source would not fully address the potential bias associated with the KED background correction. Evaluation of the KED background spectra suggests that the majority of the count rate in the traditional analysis, background-correction region of interest is unrelated to the background beneath the K-edge transmission edges. As shown in Figure 9, most of the count rate in the background region of interest is likely due to secondary scattering within the sample vial and the HKED system. The intensity and shape of this scattering contribution is dependent on the actinide concentrations within the sample as well as the interrogating x-ray intensity, so subtraction of a constant value or application of a simple scaling factor is not practical. Instead, we are working to develop a robust model to describe this scattering contribution to allow a more accurate background correction for both the traditional region of interest and for the spectral fitting methods.

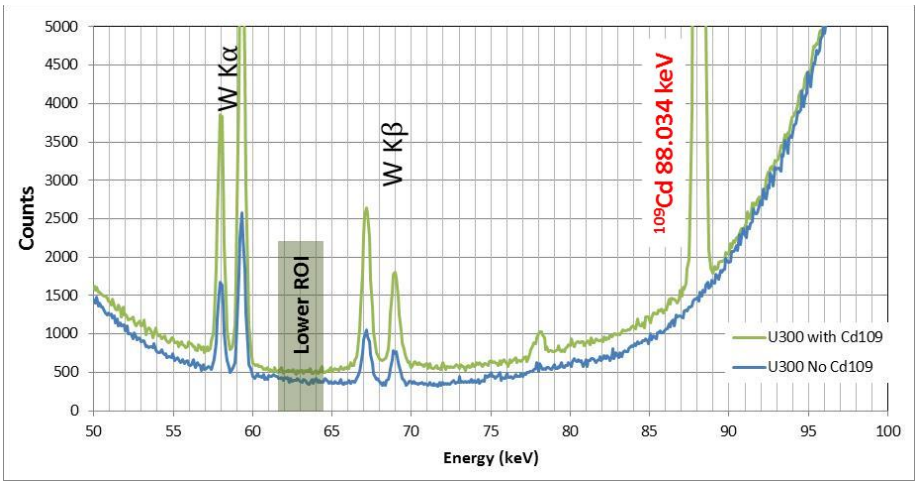

Figure 8. Measured KED transmission spectra illustrating the impact of the ^{109}Cd peak exponential tail on the lower background region of interest [9]. The large low side tail from ^{109}Cd is due to its off-axis location in close proximity to the detector and surrounded by the tungsten shield. Count rate in the 88.034 keV peak from ^{109}Cd was 153.5 cps. Note: Without the ^{109}Cd source, the count rate minimum is 70 keV, confirming that the lower region of interest includes counts other than the background.

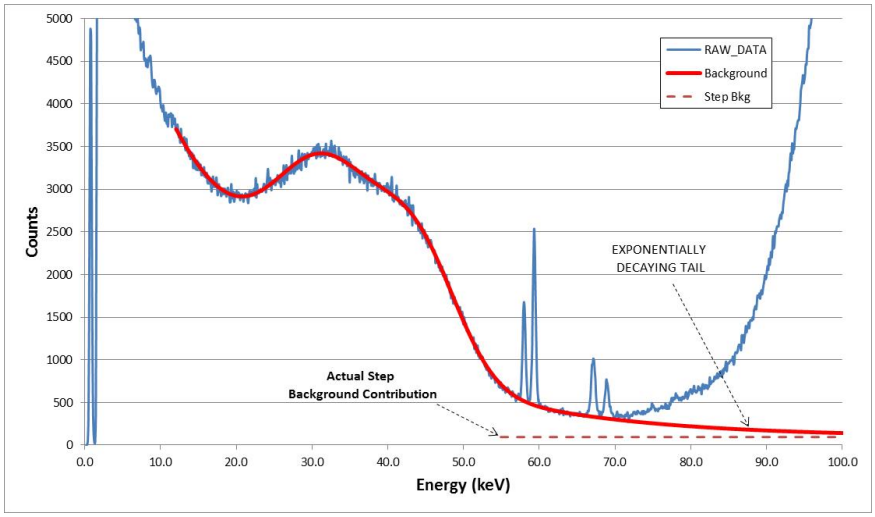

Figure 9. Low energy portion of the KED spectrum from a 321 g U/L sample without the ^{109}Cd source [9]. The solid red line represents a semiempirical fit to the data.

CONCLUSIONS

Although the HKED technique has been in use for more than 30 years, it remains an important safeguards analysis tool providing accurate near real-time analysis of the uranium and plutonium content of dissolver and product solutions produced in reprocessing of nuclear fuel. However, system performance is limited by several interferences that impact both the traditional region of interest and the more recent spectral fitting analysis methods.

Replacement of the ^{109}Cd reference source with an alternative isotope would eliminate the time-dependent biases observed in the KED transmission measurement as well as potential bias from pileup peaks impacting both the KED and XRF measurements. A suitable replacement stabilization source has not yet been identified.

An alternative self-irradiation correction, not requiring a time-consuming passive sample measurement, has been considered, but insufficient data is available to evaluate the effectiveness of the correction. The correction based on the measured fission product gamma-ray spectrum would require reconfiguring the XRF acquisition system to record energies of at least 1 MeV.

Measurement precision and accuracy of the XRF measurement can be achieved if a proper representation of the Bremsstrahlung backscatter spectrum can be developed. The continuum beneath the characteristic x-ray peaks has a structure that cannot be properly removed by region of interest or peak erosion techniques. Accurate calculation of peak area requires development of a more realistic representation of that continuum. This is particularly important if trying to quantify the minor actinide components of the solution.

The ORNL MEKED analysis, is a first principles based spectral fitting analysis method and is not impacted by the pileup or ^{109}Cd decay interferences. However, the method is performance limited by the quality of the mass attenuation coefficients and description of the low energy scatter functions. The method requires improved knowledge of the mass attenuation coefficients for the actinides over the energy range of 50 to 150 keV to fully achieve its objective of being calibration free.

REFERENCES

[1] H. Ottmar and H. Eberle, The Hybrid K-Edge/K-XRF Densitometer: Principles – Design – Performance Report, KfK 4590, Karlsruhe, 1991.

[2] R. D. McElroy, Performance Evaluation of the ORNL Multi-Elemental XRF (MEXRF) Analysis Algorithms, Report No ORNL/TM-2016/594, Oak Ridge National Laboratory, Oak Ridge, TN, 2016.

[3] R. D. McElroy Jr., S. Croft, S. L. Cleveland and G. S. Mickum, "Spectral Fitting Approach to the Hybrid K-Edge Densitometer, Preliminary Performance Results," in *Proceedings of the INMM 56th Annual Meeting*, Indian Wells, CA, USA, 2015.

[4] R. McElroy Jr., S. Cleveland, S. Croft and G. Mickum, "Relative Actinide K-Shell Vacancy Production Rates in Hybrid K-Edge Densitometry," in *37th Annual Meeting ESARDA Symposium on Safeguards and Nuclear Material Management*, Manchester, UK, May 2015.

[5] R. McElroy Jr., Performance Evaluation of the ORNL Multi-Elemental KED (MEKED) Analysis Algorithms, ORNL/TM-2018/878, Oak Ridge National Laboratory, Oak Ridge, TN, November 2018.

[6] M. Berger, J. Hubbell, S. Seltzer, J. Coursey and D. Zucker, XCOM: Photon Cross Section Database (Version 1.2), 1999. [Online]. Available: http://physics.nist.gov/xcom. [Accessed July 25, 2021].

[7] J. Hubbell, "Review of Photon Ineraction Cross Section Data in Medical and Biological Context, " *Phys. Med. Biol.,* vol. 44, pp. R2–R22, 1999.

[8] R. McElroy Jr. and S. Croft, "A Self-Irradiation Correction for the Hybrid K-Edge Densitometer, " in *Proceedings of the 60th Annual Meeting of the Institute of Nuclear Materials Management*, Palm Desert, CA, 2019.

[9] R. McElroy Jr., Performance Evaluation of the CHKED Multi-Elemental Analysis and Software, ORNL/TM-2018/867, Oak Ridge National Laboratory, Oak Ridge, TN, 2018.